

## **$^{228}\text{Ra}$ and $^{226}\text{Ra}$ Distributions off North and Southwest Taiwan**

Jeh-Chyi Yeh<sup>1</sup> and Yu-Chia Chung<sup>1</sup>

(Manuscript received 14 August 1996, in final form 9 November 1996)

### **ABSTRACT**

**A technique was developed and applied to measure  $^{228}\text{Ra}$  and  $^{226}\text{Ra}$  in seawater in the seas off north and southwest Taiwan. The method involves extraction of Ra from large-volume seawater samples with  $\text{MnO}_2$ -impregnated fiber followed by gamma-ray spectrometry using a high-purity germanium (HPGe) detector. The  $^{228}\text{Ra}$  data suggest that the surface water off north Taiwan is a mixture of about 75% Kuroshio water and 25% coastal water off mainland China if the upwelling effect is not taken into consideration. Surface water data measured in the Kaoping River and its estuary suggest that the river is not a major source of  $^{228}\text{Ra}$  and  $^{226}\text{Ra}$  in the adjacent sea. A simple one-dimensional diffusion model is not applicable to the surface water  $^{228}\text{Ra}$  data for diffusivity estimates due to variable circulation and radium sources from the north and the coasts along the Taiwan Strait. Both nuclides show a downward increase, suggesting bottom sediments as a more important source.**

**(Key words : Radium isotopes, Kuroshio, Taiwan Strait)**

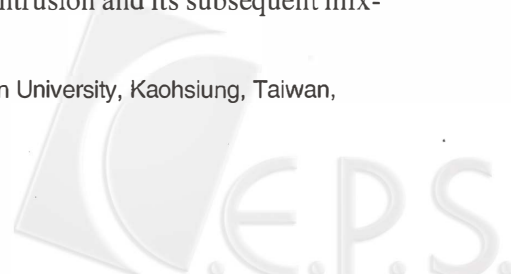
### **1. INTRODUCTION**

Since  $^{228}\text{Ra}$  in surface sea water generally decreases from the coastal-estuary zone toward the open ocean, it is regarded as a useful tracer in the study of surface water mixing and the lateral transport across marginal seas. For example,  $^{228}\text{Ra}$  was used together with salinity and silica data to trace the Amazon River component in the nearby Atlantic surface water (Moore *et al.*, 1986).

As  $^{228}\text{Ra}$  in the marginal seas off Taiwan had never been measured, it was felt that the area warranted an initial investigation. Thus, as presented in this paper, a technique to extract  $^{228}\text{Ra}$  and  $^{226}\text{Ra}$  from large-volumes of seawater with  $\text{MnO}_2$ -impregnated fiber similar to that given in the literature (e.g. Moore, 1976; Michel *et al.*, 1981; Moore *et al.*, 1985) was developed by the present authors. The Ra nuclides thereby extracted were measured by gamma-ray spectrometry using a high-purity germanium (HPGe) detector. This technique was applied to analyze water samples collected from the seas off north and southwest Taiwan. Variations in the Ra isotopes were studied in the context of the Kuroshio intrusion and its subsequent mix-

---

<sup>1</sup>Institute of Marine Geology and Chemistry, National Sun Yat-sen University, Kaohsiung, Taiwan, R.O.C.



ing with adjacent water masses. Additionally, surface water samples from the Kaoping River and its estuary were measured to determine whether the river was a major source of  $^{228}\text{Ra}$  and  $^{226}\text{Ra}$  for the adjacent sea.

## 2. METHOD

### 2.1 Sample Collection

In November, 1994, six 100-liter water samples were collected at 2 m depth with a submersible pump along a NW-SE transect off north Taiwan. Water samples of the same size were also collected in the same manner along 3 NE-SW transects off southwest Taiwan: 12 along the northern and southern transects in February, and 5 along the central one in April, 1995. At six of the stations, 100-liter samples were collected at 60 m and 200 m depths by repeated wire casts with 20-liter Go-Flo bottles in June, 1995. The station locations and sampling dates are listed in Table 1.

### 2.2 Sample Extraction

The Ra isotopes in the seawater samples were extracted by pumping through columns of Mn-impregnated fiber aboard. This Ra extraction technique coupled with measurements by gamma-ray spectrometry using a high-purity germanium detector is a frequent approach (e.g. Moore *et al.*, 1976; Michel *et al.*, 1981; Moore *et al.*, 1985) because it provides a rapid measurement by its omission of tedious chemical procedures. After repeated tests were carried out to improve extraction efficiency, the preparation of the Mn-impregnated fiber used in this study is described below.

#### 2.2.1 Preparation of the Mn-impregnated fiber

About 20 g acrylic fiber (3 denier, 10 cm long) was pre-cleaned in 6 N HCl + 1%  $\text{NH}_2\text{OHHCl}$  to reduce its radium blank, washed with distilled water several times and then immersed in a solution of 3-liter boiled 0.5 M potassium permanganate with 30 ml concentrated  $\text{H}_2\text{SO}_4$ . The solution partially oxidized the fiber onto which  $\text{MnO}_2$  was deposited. In about 30 min after the fiber was blackened throughout, it was washed with distilled water to remove excess  $\text{KMnO}_4$ . After drying, the fiber (referred to as Mn-fiber hereafter) was stored in a plastic bag for subsequent Ra extraction.

#### 2.2.2 Extraction of radium from seawater

About 20 g of the Mn-fiber was placed in a column (25 cm in length and 3 cm in diameter) for adsorption of radium isotopes onto the Mn-fiber. The seawater sample was pumped through the Mn-fiber column on deck with a flow rate of less than 0.6 l/min, as suggested by Moore (1976). After sampling, the Mn-fiber was removed from the column, rinsed with distilled water, stored in a plastic bag and returned to the shore-based laboratory for analysis.



Table 1. Locations and dates of seawater sampling for  $^{228}\text{Ra}$  and  $^{226}\text{Ra}$  measurements.

Cruise No.	Station	Date	Location	Nominal depth (m)
OR1-405C	C-1	11/06/1994	120° 30'E, 26° 20'N	2 m
	C-5	11/07/1994	121° 10'E, 26° 00'N	2 m
	C-8	11/08/1994	121° 40'E, 25° 45'N	2 m
	C-11	11/09/1994	122° 10'E, 25° 30'N	2 m
	C-14	11/10/1994	122° 40'E, 25° 15'N	2 m
	C-17	11/11/1994	123° 10'E, 25° 00'N	2 m
OR3-078	1	02/10/1995	120° 24'E, 22° 28'N	2 m
	2	02/10/1995	120° 21'E, 22° 25'N	2 m
	3	02/10/1995	120° 18'E, 22° 23'N	2 m
	4	02/10/1995	120° 10'E, 22° 15'N	2 m
	5	02/11/1995	119° 56'E, 22° 03'N	2 m
	6	02/11/1995	119° 42'E, 22° 50'N	2 m
	7	02/11/1995	119° 21'E, 22° 10'N	2 m
	8	02/11/1995	119° 18'E, 22° 24'N	2 m
	9	02/12/1995	119° 33'E, 22° 34'N	2 m
	10	02/12/1995	119° 42'E, 22° 44'N	2 m
	11	02/12/1995	120° 05'E, 22° 54'N	2 m
	12	02/12/1995	120° 08'E, 22° 40'N	2 m
OR3-091	A	04/11/1995	120° 04'E, 22° 36'N	2 m
	B	04/11/1995	119° 58'E, 22° 32'N	2 m
	C	04/11/1995	119° 52'E, 22° 26'N	2 m
	D	04/11/1995	119° 44'E, 22° 20'N	2 m
	E	04/11/1995	119° 37'E, 22° 15'N	2 m
OR3-107	5	06/11/1995	119° 56'E, 22° 03'N	60, 200 m
	8	06/11/1995	119° 18'E, 22° 24'N	60, 200 m
	9	06/11/1995	119° 33'E, 22° 34'N	60, 200 m
	10	06/12/1995	119° 42'E, 22° 44'N	60, 200 m
	B	06/12/1995	119° 58'E, 22° 32'N	60, 200 m
	E	06/12/1995	119° 37'E, 22° 15'N	60, 200 m

### 2.2.3 Leaching radium from the Mn-fiber

To remove the adsorbed radium nuclides from the Mn-fiber, it was transferred to a 2-liter glass beaker and boiled in a solution of 6 N HCl + 1%  $\text{NH}_2\text{OHHCl}$ . When the Mn-fiber turned white, the leaching was completed. The leached solution containing the radium nuclides was then transferred into a 450 ml plastic container and sealed for parent-daughter equilibration.

### 2.2.4 Determination of $^{228}\text{Ra}$ and $^{226}\text{Ra}$

The sealed solution was aged for at least one month so that  $^{228}\text{Ac}$  grew to at least 99% of  $^{228}\text{Ra}$  activity, and  $^{214}\text{Pb}$  and  $^{214}\text{Bi}$  grew to over 98% of  $^{226}\text{Ra}$  activity. The sample was then placed on top of a well-type germanium detector (Canberra Industries, Inc.) for counting. The detector had a relative efficiency of 30% and a resolution of 2.1 KeV (Full Width at Half-

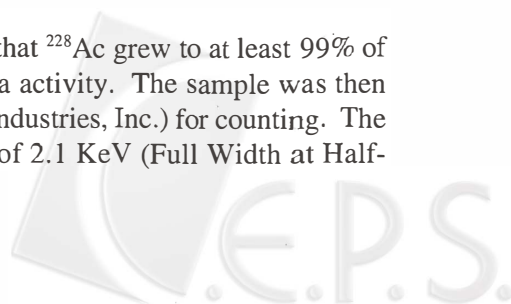


Table 2.  $^{226}\text{Ra}$  measurements by gamma-ray spectrometry on Mn-fiber extracted samples and by regenerated radon method on the same water samples for Mn-fiber extraction efficiency determination.

Sample No.	$^{226}\text{Ra}$ by gamma-ray spectrometry (dpm/100 l)	$^{226}\text{Ra}$ by regenerated radon method (dpm/100 l)	Mn-fiber extraction efficiency (%)
3-0	$11.4 \pm 2.6$	$12.8 \pm 0.3$	89
4-70	$14.5 \pm 2.7$	$16.4 \pm 0.4$	88
5-0	$11.3 \pm 2.8$	$13.4 \pm 0.3$	84
9-0	$14.5 \pm 2.3$	$16.5 \pm 0.4$	88
D-0	$9.6 \pm 1.8$	$11.0 \pm 0.2$	87
			Average = $87.2 \pm 1.9$

Maximum) at 1.33 MeV under a closed-end coaxial geometry. Each sample was counted under the same geometry for 80,000 seconds to accumulate at least 1,000 counts.

The system was calibrated with a mixed source prepared by the Taiwan Radiation Monitoring Center (TRMC) of the Atomic Energy Commission on November 14, 1994. The mixed source with nuclides of known activities was used to check the counting efficiency on a weekly basis. Based on routine bi-weekly counting data, the system blank or background was found to be quite stable.  $^{226}\text{Ra}$  was determined from the sum of the count rates at 295.2 and 352.0 KeV (due to  $^{214}\text{Pb}$ ) or from the count rate at 609.0 KeV (due to  $^{214}\text{Bi}$ ). On the other hand,  $^{228}\text{Ra}$  was determined from the sum of the count rates at 338.5, 911.1 and 968.9 KeV that were characteristic of  $^{228}\text{Ac}$  decay.

### 2.2.5 Evaluating the extraction efficiency

In order to determine the extraction efficiency of the Mn-fiber, five 120-liter size samples were collected : 100 liters for Mn-fiber extraction and gamma-ray spectrometry and the other 20 liters for  $^{226}\text{Ra}$  measurement by the regenerated radon method (Chung, 1971). Table 2 shows the  $^{226}\text{Ra}$  activities determined by the two methods along with the Mn-fiber extraction efficiency based on these data. The average extraction efficiency of  $87.2 \pm 1.9\%$  was used to correct the data obtained by the Mn-fiber extraction and gamma-ray spectrometry method. Table 3 shows the radium measurements by Mn-fiber extraction and gamma-ray spectrometry on five samples collected at the same location and at the same time. Two of the samples have no  $^{226}\text{Ra}$  data due to very low and unreliable counts of  $^{226}\text{Ra}$  daughters, but their  $^{228}\text{Ra}$  values are quite similar to those of the other samples. As fractionation of the radium isotopes caused by the extraction process is not possible, this problem remains unresolved at present. However, the reproducibility of  $^{228}\text{Ra}$  measurements is much better than expected, especially when

Table 3. Radium measurements on five identical samples by Mn-fiber extraction and gamma-ray spectrometry for reproducibility check.

Aliquot No.	$^{228}\text{Ra}$ (dpm/100 l)	$^{226}\text{Ra}$ (dpm/100 l)	$(^{228}\text{Ra}/^{226}\text{Ra})\text{A.R}$
X1	47.8±3.2	15.7±1.9	3.04±0.42
X2	47.4±3.3	16.3±4.2	2.92±0.78
X3	48.2±4.3	-	
X4	48.7±4.9	15.9±2.5	3.06±0.57
X5	47.9±5.3	-	
Average	48.0±0.5	16.0±0.3	3.01±0.08

- : not detected

Table 4.  $^{228}\text{Ra}$ ,  $^{226}\text{Ra}$  and activity ratio in the surface seawater off north Taiwan.

Station No.	Salinity (psu)	$^{228}\text{Ra}$ (dpm/100 l)	$^{226}\text{Ra}$ (dpm/100 l)	$(^{228}\text{Ra}/^{226}\text{Ra})\text{A.R}$
C-1	32.14	63.6±4.4	13.9±1.9	4.58±0.70
C-5	33.98	16.3±3.6	14.0±2.1	1.16±0.31
C-8	34.36	16.3±3.7	9.3±1.8	1.75±0.52
C-11	34.44	25.8±3.3	14.8±2.1	1.74±0.33
C-14	34.59	13.2±3.3	11.1±1.9	1.19±0.36
C-17	34.53	-	10.1±1.6	

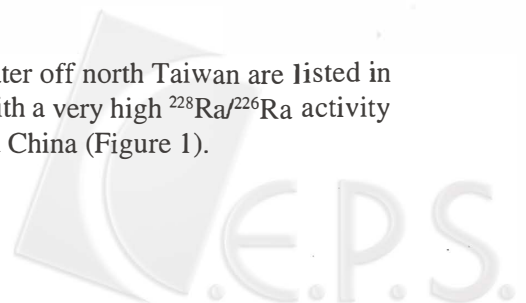
- : not detected

the uncertainty of each individual value is considered. This is also true for  $^{226}\text{Ra}$  which has an even larger relative uncertainty in gamma counting.

### 3. RESULTS AND DISCUSSION

#### 3.1 Radium Distribution off North Taiwan in Winter

$^{228}\text{Ra}$ ,  $^{226}\text{Ra}$  and their activity ratio in the surface seawater off north Taiwan are listed in Table 4 together with salinity. Very high  $^{228}\text{Ra}$  associated with a very high  $^{228}\text{Ra}/^{226}\text{Ra}$  activity ratio is observed only at C-1, the station closest to mainland China (Figure 1).



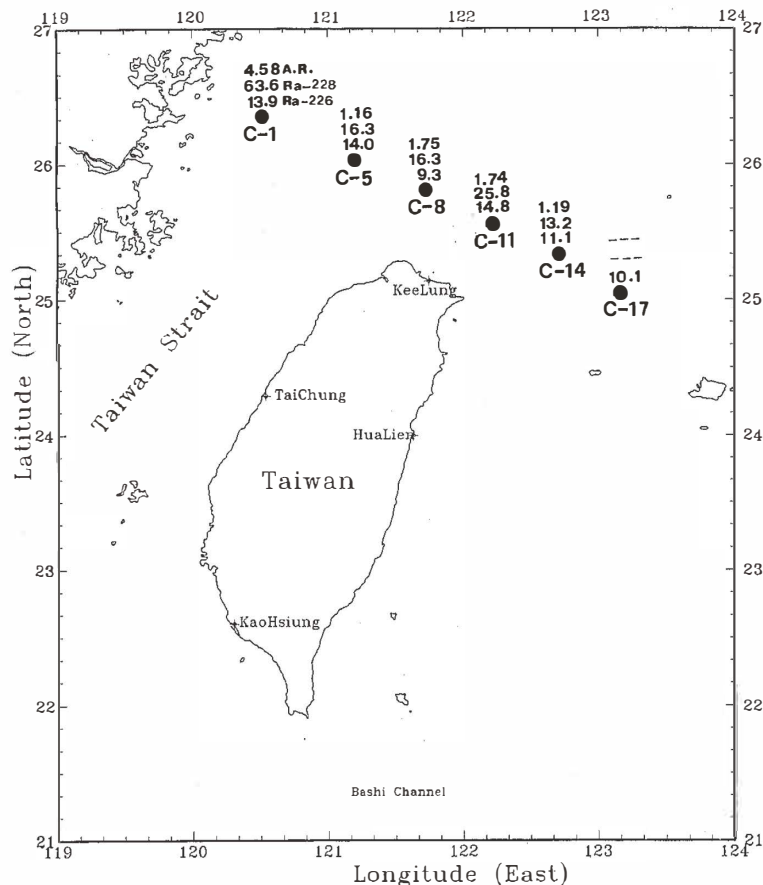


Fig. 1.  $^{228}\text{Ra}$ ,  $^{226}\text{Ra}$  and the activity ratio in the surface water along the NW-SE transect off north Taiwan.

At Station C-11, where an upwelling center is located (Liu *et al.*, 1992), both  $^{228}\text{Ra}$  and  $^{226}\text{Ra}$  are higher than at its neighboring stations, suggesting an input from deeper layers by the Kuroshio upwelling.  $^{226}\text{Ra}$  activities observed in this study are higher than those of Chung and Yin (1995), probably reflecting both hydrographic variations and a state of vertical mixing which is more rigorous in winter when the northeast monsoon prevails.

If the surface water  $^{228}\text{Ra}$  concentration of the Kuroshio (2.5 dpm/100l, Nozaki *et al.*, 1989) and that of the station closest to the mainland (63.6 dpm/100l) are adopted as the two end-member values for mixing, then the mean concentration of about 18 dpm/100l for stations located in between should correspond to a mixture of about 75 % Kuroshio water and 25 % coastal water. If the high value observed at the upwelling site (C-11) is excluded from the mean, then the Kuroshio water will account for an even higher proportion of the mixture. This is consistent with the observations that the Kuroshio water intrudes onto the shelf sea north of Taiwan (Liu *et al.*, 1992).

Table 5.  $^{228}\text{Ra}$ ,  $^{226}\text{Ra}$  and activity ratio in the surface seawater off southwest Taiwan including Kaoping River.

Station No.	Salinity (psu)	$^{228}\text{Ra}$ (dpm/100 l)	$^{226}\text{Ra}$ (dpm/100 l)	$(^{228}\text{Ra}/^{226}\text{Ra})\text{A.R}$
OR 3 Cruise 078 (2/10-2/12/1995) : winter				
1	34.39	27.1±3.2	19.8±3.3	1.37±0.28
2	34.47	28.7±4.3	13.2±1.5	2.17±0.41
3	34.65	28.1±3.3	12.9±1.7	2.18±0.38
4	34.51	15.1±3.2	11.2±2.2	1.35±0.39
5	34.51	8.0±3.2*	12.8±2.7	0.63±0.28*
6	34.51	17.5±2.8	12.0±2.7	1.46±0.40
7	34.53	26.2±3.1	12.5±2.5	2.11±0.49
8	34.36	36.4±3.6	21.8±2.8	1.67±0.27
9	34.31	32.4±3.5	16.4±2.2	1.98±0.34
10	34.42	23.4±3.2	14.5±1.6	1.61±0.28
11	34.71	18.4±3.8	11.8±2.5	1.56±0.46
12	34.68	24.6±3.2	-	
OR 3 Cruise 091 (4/11/1995) : spring				
A	34.58	22.6±3.6	16.0±2.3	1.41±0.30
B	34.54	23.0±3.9	9.8±1.2	2.35±0.49
C	34.56	16.5±2.0	10.5±1.7	1.57±0.32
D	34.44	29.1±4.3	10.8±1.8	2.69±0.60
E	34.45	27.6±4.1	14.5±2.2	1.90±0.40
Surface water in Kaoping River				
S-0	0	25.9±3.3	13.6±1.5	1.91±0.32
S-3	3	22.9±2.7	18.9±1.9	1.22±0.19
S-10	10	20.1±3.6	17.1±1.8	1.17±0.24
S-20	20	30.3±3.0	19.4±1.9	1.58±0.22

- : not detected

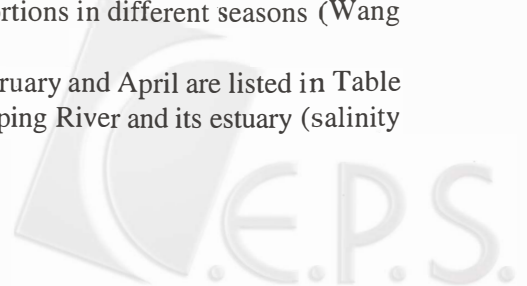
\* : questionable value

### 3.2 Radium Distributions off Southwest Taiwan

#### 3.2.1 Surface water $^{228}\text{Ra}$ and $^{226}\text{Ra}$ in winter and spring

At the sea off southwest Taiwan, the hydrography reflects the effects of the northeast and southwest monsoons, bottom topography, the Kuroshio intrusion and several coastal currents (Fan, 1982 and 1984). Three major water masses are recognized in the area: the coastal water off mainland China, the Kuroshio water and the surface water from the South China Sea. The mixing of these water masses may occur in variable proportions in different seasons (Wang and Chern, 1988; Shaw, 1991).

The surface water  $^{228}\text{Ra}$  and  $^{226}\text{Ra}$  data obtained in February and April are listed in Table 5. Included in the table are the data obtained from the Kaoping River and its estuary (salinity





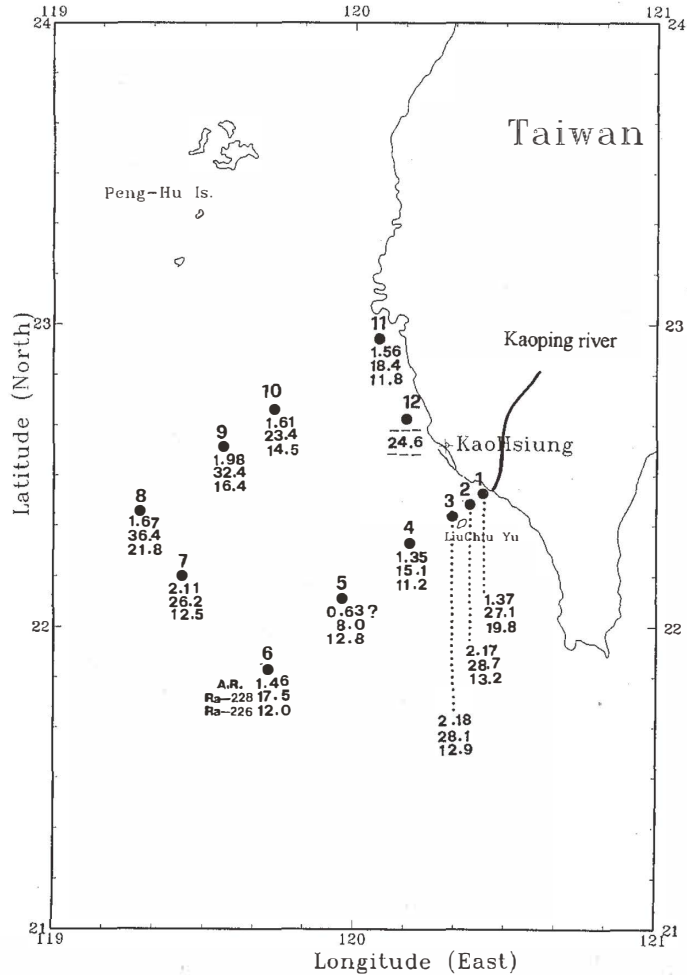
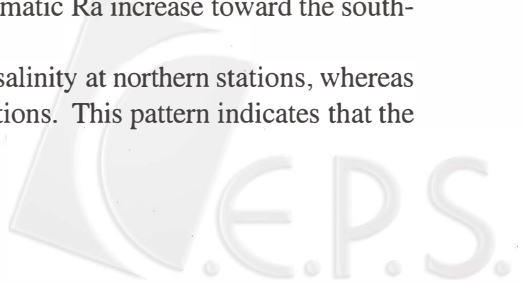


Fig. 2.  $^{228}\text{Ra}$ ,  $^{226}\text{Ra}$  and the activity ratio in the surface water off southwest Taiwan in February, 1995.

from 0 to 20 psu). Both nuclides increase generally toward the north and the west, with the maximum at the northwest corner (Station 8, Figure 2). Along the northern NE-SW transect,  $^{228}\text{Ra}$  and  $^{226}\text{Ra}$  increase from 18.4 and 11.8 dpm/100l at Station 11 to 36.4 and 21.8 dpm/100l at Station 8, respectively. They also increase northwestward from Station 6 to Station 8. At the southern NE-SW transect, they are higher only in the coastal water near the Kaoping River which is probably partly due to desorption of Ra from the sediments resuspended at the estuary. As the  $^{228}\text{Ra}$  value at Station 5 is questionable, a systematic Ra increase toward the southwest cannot be established.

High radium activity is generally correlated with low salinity at northern stations, whereas low activity is correlated with high salinity at southern stations. This pattern indicates that the





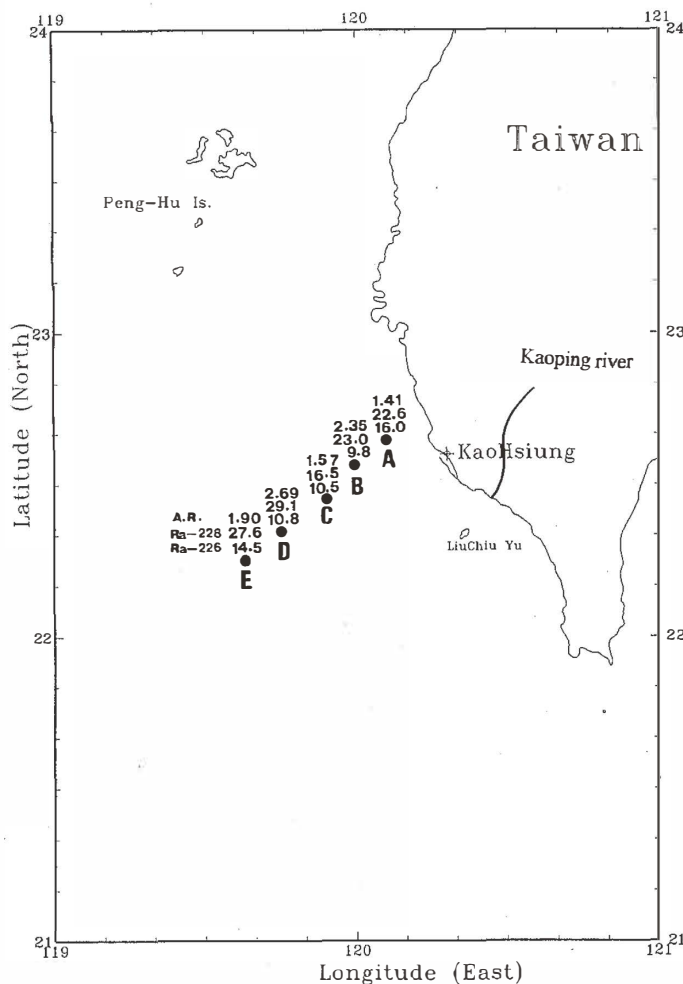


Fig. 3.  $^{228}\text{Ra}$ ,  $^{226}\text{Ra}$  and the activity ratio in the surface water off southwest Taiwan in April, 1995.

low salinity coastal water of high radium concentrations can contribute  $^{228}\text{Ra}$  and  $^{226}\text{Ra}$  to the study area, while the high salinity Kuroshio water of low radium concentrations can dilute the nuclide concentrations in the area. Since the concentrations of the nuclides in the Kaoping River and in the river discharge area (Stations 1 to 3) are generally lower than those in the Taiwan Strait water, the Kaoping River cannot be a major source for the surface water radium off southwest Taiwan, especially in winter when the river discharge is low. On the contrary, a major source for the surface water radium in the study area during winter is probably the high radium coastal water from the north which is driven southward by the northeast monsoon (Wang and Chern, 1988). Along the central NE-SW transect in spring, the surface water radium nuclides show no clear trend and have values in between those of the northern and southern transects (Figures 2 and 3).

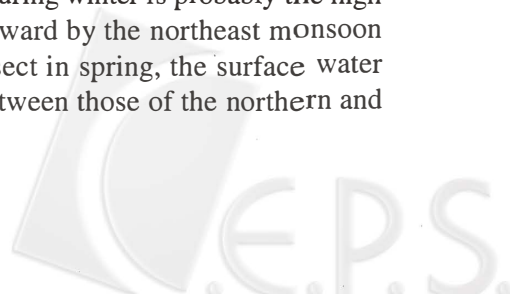


Table 6.  $^{228}\text{Ra}$ ,  $^{226}\text{Ra}$  and activity ratio in the seawater collected at 60 m and 200 m depth off southwestern Taiwan in June, 1995.

Station No.	Bottom depth (m)	Nominal depth (m)	$^{228}\text{Ra}$ (dpm/100 l)	$^{226}\text{Ra}$ (dpm/100 l)	$(^{228}\text{Ra}/^{226}\text{Ra})\text{A.R.}$
B	627	60	$16.4 \pm 3.6$	$13.6 \pm 2.6$	$1.21 \pm 0.35$
		200	$24.0 \pm 3.8$	$17.9 \pm 2.6$	$1.34 \pm 0.29$
E	1500	60	$17.8 \pm 2.8$	$11.8 \pm 2.0$	$1.51 \pm 0.35$
		200	$24.6 \pm 3.9$	$14.6 \pm 1.1$	$1.68 \pm 0.29$
5	1037	60	$18.4 \pm 2.7$	$12.5 \pm 1.7$	$1.47 \pm 0.29$
		200	$18.4 \pm 2.3$	$13.7 \pm 2.2$	$1.34 \pm 0.27$
8	210	60	$19.7 \pm 2.9$	$13.8 \pm 1.4$	$1.43 \pm 0.26$
		200	$21.0 \pm 3.6$	$19.6 \pm 1.8$	$1.07 \pm 0.21$
9	230	60	$21.4 \pm 3.0$	$16.0 \pm 1.5$	$1.34 \pm 0.23$
		200	$26.1 \pm 5.5$	$21.9 \pm 3.3$	$1.19 \pm 0.31$
10	203	60	$18.5 \pm 2.5$	$12.7 \pm 1.8$	$1.46 \pm 0.29$
		200	$22.5 \pm 4.1$	$23.0 \pm 2.1$	$0.98 \pm 0.20$

The  $^{228}\text{Ra}/^{226}\text{Ra}$  activity ratio varies from 1.35 to 2.18 in winter, and from 1.41 to 2.69 in spring (Table 5, Figures 2 and 3). Along the NW-SE transect off north Taiwan, the activity ratio has comparable values except at the coastal station (C-1 in Figure 1). Since the hydrography indicates that the mixing of several water masses with different proportions occurs in different seasons, a steady-state mixing model is not applicable to the  $^{228}\text{Ra}$  data for mixing rate estimates in the area.

### 3.2.2 $^{228}\text{Ra}$ and $^{226}\text{Ra}$ at 60 m and 200 m depth in summer

At six of the stations off southwest Taiwan, seawater samples at 60 m and 200 m depths were collected in June, 1995. Radium isotopes in each sample of about 100 liters were extracted by the Mn-fiber on deck and processed in the laboratory for gamma counting in the same manner as that for surface waters. The data are presented in Table 6. Albeit with large uncertainties, both  $^{228}\text{Ra}$  and  $^{226}\text{Ra}$  are generally higher at the depth of 200 m than at 60 m.

Earlier hydrographic studies have shown that a branch of the warm and saline Kuroshio water flows from the Bashi Channel and the study area into the Taiwan Strait in the upper 150 m during winter (Fan, 1982 and 1984; Wang and Chern, 1988; Shaw, 1991). However, the area is occupied by the warm but less saline water mainly of the South China Sea during summer as indicated by hydrography (Fan, 1984), and the upper 60 m layer is well mixed.

$^{228}\text{Ra}$ ,  $^{226}\text{Ra}$  and the activity ratio at 60 m depth are fairly uniform (Figure 4) but are somewhat higher at the northern stations than at the southern ones, probably because the former are closer to the source from the north and also shallower and so much closer to the source from the bottom sediments than the latter. The diffusion of radium from the bottom sediments may be responsible for the observed higher concentrations at a greater (200 m) depth (Figure 4).

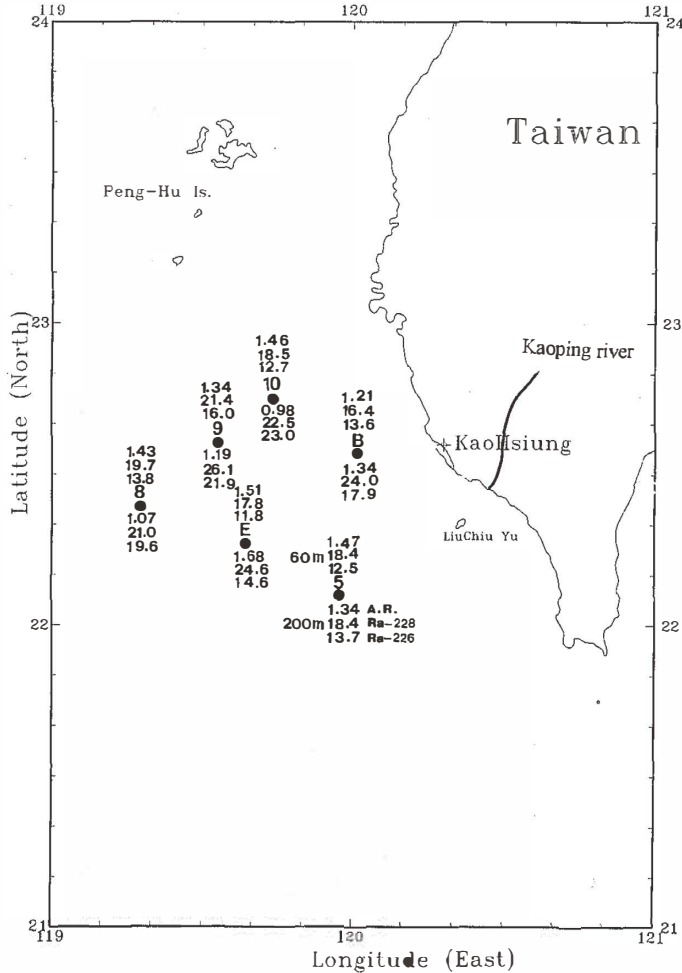
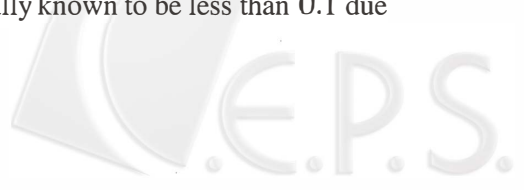


Fig. 4.  $^{228}\text{Ra}$ ,  $^{226}\text{Ra}$  and the activity ratio in the subsurface water (60 m and 200 m) off southwest Taiwan in June, 1995.

Figure 5 shows plots of  $^{228}\text{Ra}$  versus  $^{226}\text{Ra}$  for all the data obtained from this study and some surface water data from the northern East China Sea (Nozaki *et al.*, 1989), the South China Sea (Huang *et al.*, 1996) and the North Pacific (Yamada and Nozaki, 1986). Clearly, three domains of distribution are observed : (1) high activity ratios of about 4 in the coastal surface waters of the East China Sea and the South China Sea due to a relatively high  $^{228}\text{Ra}$  source in the coastal areas; (2) low activity ratios of much less than 1 in the North Pacific surface water; and (3) moderate activity ratios of usually between 1 and 2 as observed in marginal seas, such as in the study areas. Such moderate values may have resulted from a mixture of the two extrema plus from, perhaps, additional input from the nearby land masses. In the deep open ocean, the activity ratios are characteristically known to be less than 0.1 due



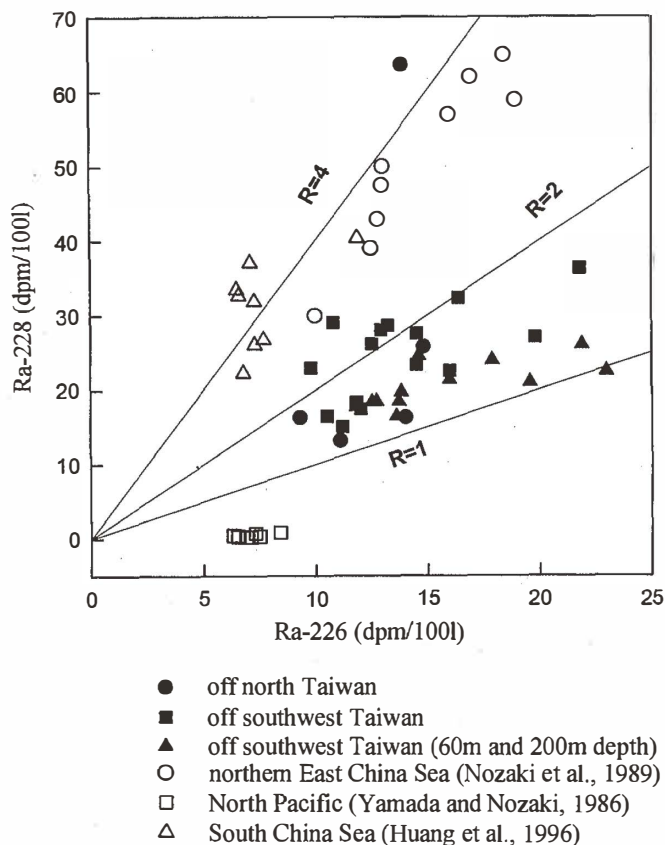


Fig. 5.  $^{228}\text{Ra}$  vs  $^{226}\text{Ra}$  plots for surface waters at coastal zones, marginal seas and open ocean. Those for the subsurface water off southwest Taiwan are also included.

to the absence of Ra contribution from land masses.

#### 4. CONCLUSIONS

It is extremely important that the analytical methods for radium measurements by gamma-ray spectrometry be improved so that better quality data can be obtained. The radium extraction efficiency by the Mn-fiber is about 87 %, which is somewhat less than satisfactory. To reduce the number of errors in gamma-ray spectrometry, the size of samples should be enlarged and a high-efficiency gamma-ray detector should be used.

$^{228}\text{Ra}$  and  $^{228}\text{Ra}/^{226}\text{Ra}$  activity ratio in the surface seawater off north Taiwan are clearly much higher at the station closest to mainland China ( $^{228}\text{Ra}$  at 63.3 dpm/100l and activity ratio at 4.58) than at other stations far away from the mainland. Along the NW-SE transect to the Kuroshio, both the  $^{228}\text{Ra}$  and the activity ratio are lower due to mixing with the Kuroshio water ( $^{228}\text{Ra}$  at 13.2 dpm/100l and the ratio at 1.19 at the southeast station, C-14). If the surface

water  $^{228}\text{Ra}$  concentration of the Kuroshio and that of the nearshore southern East China Sea are adopted as the two end-member values and the contribution by upwelling is not considered, then the surface water along the transect should be composed of about 75 % Kuroshio water and about 25 % nearshore surface water of mainland China.

In the area off southwest Taiwan, the surface water  $^{228}\text{Ra}$  and  $^{226}\text{Ra}$  distributions in winter support the Kuroshio water intrusion :  $^{228}\text{Ra}$  and  $^{226}\text{Ra}$  increase northward and westward rather than eastward to the Taiwan coast except at the estuarine stations. Radium maxima are observed at the station to the northwest corner (36.4 dpm/100l for  $^{228}\text{Ra}$ ; 21.8 dpm/100l for  $^{226}\text{Ra}$ ), indicative of the greatest influence of the mainland nearshore water (Figure 2). Radium in the spring surface water along the NE-SW transect (Figure 3) increases somewhat toward the west, similar to that in the winter surface water. Since the Ra concentrations in the Kaoping River are lower than those in the Taiwan Strait water, the Kaoping River cannot be a major Ra source for the surface seawater off southwest Taiwan. This leads to the conclusion that the major Ra source for the surface water in the area during winter is most likely the mainland coastal water from the north which, with a high Ra concentration, is driven southward by the northeast monsoon.

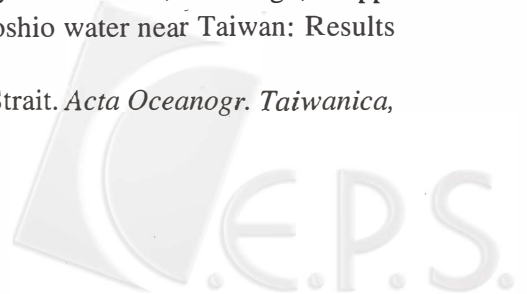
Ra isotopes at 60 m are fairly uniform, indicating that the water at this depth and above is probably well mixed in summer. The activities at 200 m are all higher than at 60 m, implying a significant contribution from bottom sediments. As the hydrography and circulation in the study area vary seasonally with the monsoons, the  $^{228}\text{Ra}$  and  $^{228}\text{Ra}/^{226}\text{Ra}$  activity ratio may change accordingly. Therefore, they are not applicable to mixing rate estimates.

The  $^{228}\text{Ra}/^{226}\text{Ra}$  activity ratios observed in the study areas usually fall between 1 and 2 with only a few values greater than 2 (Figure 5). These values are in between those of the open ocean surface water (< 1) and those of the East China Sea and South China Sea coastal surface waters (~ 4) and may indeed represent a mixture of the two extrema in a marginal sea environment.

**Acknowledgments** The authors are grateful for the courtesy offered by Mr. S.Y. Lin in providing the acrylic fiber for the experiment. Marine technicians and the crew of the R/V Ocean Researcher I and III were very helpful during sample collections. Thanks are also due to members of the Radioisotope Lab of the Institute of Marine Geology and Chemistry, National Sun Yat-sen University, on various phases of this work. The financial support was provided by the National Science Council, Taiwan, R.O.C. under grants NSC 82-0209-M-110-043K, NSC 83-0209-M-110-011-K, and NSC 84-2611-M-110-002-K2.

## REFERENCES

- Chung, Y., 1971 : Pacific deep and bottom water studies based on temperature, radium and excess-radon measurements. Ph. D. Thesis, University of California, San Diego, 139pp.
- Chung, Y. and H.C. Yin, 1995 : Radium-226 in the Kuroshio water near Taiwan: Results from the KEEP-MASS programs. *TAO*, **6**, 47-63.
- Fan, K.L., 1982 : A study of water masses in the Taiwan Strait. *Acta Oceanogr. Taiwanica*, **13**, 140-153.



- Fan, K.L., 1984 : The branch of the Kuroshio in the Taiwan Strait. In: T. Ichiye (Ed.), Ocean hydrodynamics of the Japan and East China Seas, Elsevier, New York, 77-82.
- Huang, Y., Y. Xie, M. Chen, F. Chen and Y. Qiu, 1996 : Distribution feature of  $^{228}\text{Ra}$  in surface seawater of the Nansha Sea area. In: Isotope marine chemistry of the Nansha Island waters, China Ocean Press, Beijing, 70-78, (in Chinese with English abstract).
- Liu, K.K., G.C. Gong, C.Z. Shyu, S.C. Pai, C.L. Wei and S.Y. Chao, 1992 : Response of Kuroshio upwelling to the onset of the northeast monsoon in the sea north of Taiwan : Observations and a numerical simulation. *J. Geophys. Res.*, **97**, 12511-12526.
- Michel, J., W.S. Moore and P.T. King, 1981 : Gamma-ray spectrometry for determination of radium-228 and radium-226 in nature waters. *Anal. Chem.*, **53**, 1885-1889.
- Moore, W.S. 1976 : Sampling  $^{228}\text{Ra}$  in the deep ocean. *Deep-Sea Res.*, **23**, 647-651.
- Moore, W.S., R.M. Key and J.L. Sarmiento, 1985 : Techniques for precise mapping of  $^{226}\text{Ra}$  and  $^{228}\text{Ra}$  in the ocean. *J. Geophys. Res.*, **90**, 6983-6994.
- Moore, W.S., J.L. Sarmiento and R.M. Key, 1986 : Tracing the Amazon component of surface Atlantic water using  $^{228}\text{Ra}$ , salinity and silicon. *J. Geophys. Res.*, **91C**, 2574-2580.
- Nozaki, Y., V. Kasemsupaya and H. Tsubota, 1989 : Mean residence time of the shelf water in the East China and Yellow Seas determined by  $^{228}\text{Ra}/^{226}\text{Ra}$  measurements. *Geophys. Res. Lett.*, **16**, 1297-1300.
- Shaw, P.T., 1991 : The intrusion of water masses into the sea southwest of Taiwan. *J. Geophys. Res.*, **94**, 18213-18226.
- Wang, J. and C.S. Chern, 1988 : On the Kuroshio branch in the Taiwan Strait during winter-time. *Acta Oceanogr. Taiwanica*, **21**, 469-491.
- Yamada, M. and Y. Nozaki, 1986 : Radium isotopes in coastal and open ocean surface waters of the western North Pacific. *Mar. Chem.*, **19**, 379-389.

